



# $K^+/NH_4^+$ antiporter: a unique ammonium carrying transporter in the kidney inner medulla

Hassane Amlal, Manoocher Soleimani \*

Department of Medicine, University of Cincinnati School of Medicine, and Veterans Affairs Medical Center, Cincinnati, OH 45267-585, USA

Received 9 July 1996; accepted 17 September 1996

## Abstract

The mechanism of  $NH_4^+$  transport in inner medulla is not known. The purpose of these experiments was to study the process that is involved in ammonium ( $NH_4^+$ ) transport in cultured inner medullary collecting duct (mIMCD-3) cells. Cells grown on coverslips were exposed to  $NH_4^+$  and monitored for  $pH_i$  changes by the use of the pH-sensitive dye BCECF. The rate of cell acidification following the initial cell alkalization was measured as an index of  $NH_4^+$  transport. The rate of  $NH_4^+$  transport was the same in the presence or absence of sodium in the media ( $0.052 \pm 0.003$  vs.  $0.048 \pm 0.004$  pH/min,  $P > 0.05$ ), indicating that  $NH_4^+$  entry into the cells was independent of sodium. The presence of ouabain, bumetanide, amiloride, barium, or 4,4'-di-isothiocyanostilbene-2-2'-disulfonic acid (DIDS) did not block the  $NH_4^+$ -induced cell acidification, indicating lack of involvement of  $Na^+:K^+$ -ATPase,  $Na^+:K^+:2Cl^-$  transport,  $Na^+:H^+$  exchange,  $K^+$  channel, or  $Cl^-$ /base exchange, respectively, in  $NH_4^+$  transport. The  $NH_4^+$ -induced cell acidification was significantly inhibited in the presence of high external  $[K^+]$  as compared to low external  $[K^+]$  ( $0.018 \pm 0.001$  vs.  $0.049 \pm 0.003$  pH/min for 140 mM  $K^+$  vs. 1.8 mM  $K^+$  in the media, respectively,  $P < 0.001$ ). Inducing  $K^+$  efflux by imposing an outward  $K^+$  gradient caused intracellular acidification by  $\sim 0.3$  pH unit in the presence but not the absence of  $NH_4^+$ . This  $K^+$  efflux-induced  $NH_4^+$  entry increased by extracellular  $NH_4^+$  in a saturable manner with a  $K_m$  of  $\sim 5$  mM, blocked by increasing extracellular  $K^+$  and was not inhibited by barium. The  $K^+$  efflux-coupled  $NH_4^+$  entry was electroneutral as monitored by the use of cell membrane potential probe 3,3'-dipropylthiadicarbocyanine. These results are consistent with the exchange of internal  $K^+$  with external  $NH_4^+$  in a 1:1 ratio. The  $K^+-NH_4^+$  antiporter was inhibited by verapamil and Schering 28080 in a dose-dependent manner, was able to work in reverse mode, and did not show any affinity for  $H^+$  as a substrate, indicating that it is distinct from other  $NH_4^+$ -carrying transporters.

We conclude that a unique transporter, a potassium-ammonium ( $K^+/NH_4^+$ ) antiport, is responsible for  $NH_4^+$  transport in renal inner medullary collecting duct cells. This antiporter is sensitive to verapamil and Schering 28080, is electroneutral, and is selective for  $NH_4^+$  and  $K^+$  as substrates. The  $K^+/NH_4^+$  antiporter may play a significant role in acid-base regulation by excretion of ammonium and elimination of acid.

**Keywords:** Inner medulla;  $NH_4^+$ ;  $K^+$ ; Antiporter; Acid-base

## 1. Introduction

Excretion of  $NH_4^+$  by the kidney is essential to acid-base regulation in mammalian species [1]. Stud-

\* Corresponding author. Fax: +1 513 5584309.

ies in nephron segments have demonstrated that  $\text{NH}_4^+$  is secreted into the lumen of proximal tubule [1,2], reabsorbed in the medullary thick ascending limb [1,3], and transported to the medullary collecting duct cells where it is secreted into the lumen down a favorable  $\text{NH}_3$  concentration gradient [4–6]. Micro-perfusion and influx experiments have illustrated that secretion of newly-synthesized  $\text{NH}_4^+$  into the lumen of proximal tubule (PT) is predominantly mediated via  $\text{Na}^+/\text{H}^+$  exchanger [7,8]. The reabsorption of  $\text{NH}_4^+$  in the lumen of medullary thick ascending limb of Henle (mTAL) occurs mostly via  $\text{Na}^+:\text{K}^+:\text{2Cl}^-$  cotransport [9–12]. While it has been shown that inner medullary collecting duct (IMCD) is the major segment for secretion of  $\text{NH}_4^+$  [1,4–6], the cellular mechanism mediating the transport of  $\text{NH}_4^+$  from the interstitium to the medullary collecting duct cells remains unknown. Insight into the cellular mechanism of  $\text{NH}_4^+$  transport in this nephron segment would likely increase our understanding regarding a variety of pathologic conditions associated with acid-base abnormalities.

Because of similarities between  $\text{K}^+$  and  $\text{NH}_4^+$  structure [4],  $\text{NH}_4^+$  may substitute for potassium in several transport processes [9–13]. Amongst these transporters,  $\text{Na}^+:\text{K}^+:\text{2Cl}^-$  cotransport and  $\text{Na}^+:\text{K}^+:\text{ATPase}$  are two known examples [9–13]. Studies in rat kidney have shown that the rate of  $\text{NH}_4^+$  reabsorption in the mTAL lumen is affected by  $\text{K}^+$  concentration, indicating competition of  $\text{NH}_4^+$  and  $\text{K}^+$  for the same binding site in luminal  $\text{Na}^+:\text{K}^+:\text{2Cl}^-$  cotransporter [9,10]. The interaction of  $\text{NH}_4^+$  with the  $\text{Na}^+:\text{K}^+:\text{ATPase}$  is less well documented:  $\text{NH}_4^+$  has been shown to have affinity for the  $\text{Na}^+:\text{K}^+:\text{ATPase}$  in rabbit proximal tubules [14] but not in the opossum kidney cells [15]. In rat IMCD cells [13] or mouse IMCD cells [16]  $\text{NH}_4^+$  can decrease ouabain-sensitive or bumetanide-sensitive  $^{86}\text{Rb}$  influx, suggesting interaction of  $\text{NH}_4^+$  with the  $\text{K}^+$  site of  $\text{Na}^+:\text{K}^+:\text{ATPase}$  or basolateral  $\text{Na}^+:\text{K}^+:\text{2Cl}^-$  transporter, respectively. These studies [13,16], however, did not measure  $\text{NH}_4^+$  transport. As such, the contribution of  $\text{Na}^+:\text{K}^+:\text{ATPase}$  or basolateral  $\text{Na}^+:\text{K}^+:\text{2Cl}^-$  transporter to total  $\text{NH}_4^+$  transport in rat or mouse IMCD cells was not determined.  $\text{NH}_4^+$  can also compete with  $\text{K}^+$  binding site on  $\text{K}^+$  channel [15,17]. Recent studies in cell suspensions from thick ascending limb of rat kidney showed that  $\text{NH}_4^+$  could

be transported on  $\text{K}^+/\text{H}^+$  antiport [18] and  $\text{K}^+:\text{Cl}^-$  cotransport [12].

In the present work, we studied  $\text{NH}_4^+$  transport in cultured mouse IMCD cells by monitoring  $\text{pH}_i$ . Cells were exposed to varying  $\text{NH}_4^+$  concentrations and the rate of cell acidification following the initial cell alkalinization was then measured as an index of  $\text{NH}_4^+$  transport. This cell acidification was only observed in the presence of  $\text{NH}_4^+$  and was not mediated via known transporters that interact with  $\text{NH}_4^+$ . The results provide evidence for the presence of a new transporter, called here  $\text{K}^+/\text{NH}_4^+$  antiporter, which is responsible for majority of  $\text{NH}_4^+$  transport in mIMCD-3 cells. This transporter exchanges intracellular  $\text{K}^+$  with extracellular  $\text{NH}_4^+$  and is likely responsible for the transport of  $\text{NH}_4^+$  from the interstitium to the cells of inner medullary collecting duct. The  $\text{K}^+/\text{NH}_4^+$  antiport may play an essential role in  $\text{NH}_4^+$  excretion into the urine and thus regulation of acid base.

## 2. Materials and methods

### 2.1. Cell culture procedures

mIMCD-3 cells were cultured in a 1:1 mixture of Ham's F-12 and Dulbecco's modified Eagle's medium (DME) containing 100 U/ml penicillin-G and supplemented with 10% fetal bovine serum as described [19]. The mIMCD-3 cell line which has been developed from simian virus transgenic mice retains many characteristics of this nephron segment [20]. Cultured cells were incubated at 37°C in a humidified atmosphere of 5%  $\text{CO}_2$  in air. The medium was replaced every other day.

### 2.2. Intracellular pH measurement

Changes in intracellular pH ( $\text{pH}_i$ ) were monitored using the acetoxymethyl ester of the pH-sensitive fluorescent dye 2',7'-bis (carboxyethyl)-5(6)-carboxy-fluorescein (BCECF-AM) as described [18,19,21,22]. mIMCD-3 cells were grown to confluence on coverslip and incubated in the presence of 5  $\mu\text{M}$  BCECF in a solution consisting of 140 mM NaCl, 0.8 mM  $\text{K}_2\text{HPO}_4$ , 0.2 mM  $\text{KH}_2\text{PO}_4$ , 1 mM  $\text{CaCl}_2$ , 1 mM  $\text{MgCl}_2$ , 10 mM Hepes (*N*-2-hydroxyethylouoera-

Table 1  
Composition of experimental solutions

Compound	Solutions			
	A	B	C	D
NaCl	140			
KCl			140	1.8
TMA-Cl		140		125
K <sub>2</sub> HPO <sub>4</sub>	0.8	0.8	0.8	
KH <sub>2</sub> PO <sub>4</sub>	0.2	0.2	0.2	
CaCl <sub>2</sub>	1	1	1	1
MgCl <sub>2</sub>	1	1	1	1
Hepes	10	10	10	10
Glucose	5	5	5	5
Barium				10

Concentrations are in mM. All solutions were bubbled with 100% O<sub>2</sub> and adjusted to pH 7.40.

zube-*N'*-2-ethanesulfonic acid) and 5 mM glucose (solution A, Table 1). To measure the intracellular pH, each coverslip was positioned diagonally in a cuvette and the latter was then placed in a thermostatically controlled holding chamber (37°C) in a Delta Scan dual excitation spectrofluorometer (PTI, double-beam fluorometer, Photon Technology International, Brunswick, NJ). The monolayer was then perfused with the appropriate solution (Table 1). The perfusion was achieved using a Harvard constant infusion pump. Where indicated, inhibitors or their vehicles were added to the experimental solution in a 1:1000 dilution from a stock solution. The fluorescence ratio at excitation wavelengths of 500 and 450 nm was utilized to determine intracellular pH values in the experimental groups by comparison to the calibration curve. The emission wavelength was recorded at 525 nm. The calibration curve was generated using KCl/nigericin technique and solutions of varying pH. The experiments were performed in iso-osmotic CO<sub>2</sub>-free media buffered with Hepes. To measure the rate of NH<sub>4</sub><sup>+</sup> transport, cells were exposed to an NH<sub>4</sub><sup>+</sup>-containing solution. The rate of cell acidification (dpH<sub>i</sub>/dt) following the initial alkalization was measured as an index of NH<sub>4</sub><sup>+</sup> flux into the cells; this is an established method used by several investigators to determine the rate of NH<sub>4</sub><sup>+</sup> transport into cells of various tissues [12,18]. Initial rates of cell acidification (dpH<sub>i</sub>/dt) were estimated from the slopes of pH<sub>i</sub> vs. time (*t*) and were ex-

pressed as pH units per minutes. Correlation coefficients for these linear fits averaged  $0.976 \pm 0.004$ .

### 2.3. Preparation of mIMCD-3 cell suspension

mIMCD-3 cells were grown to confluence in 75 cm<sup>2</sup> flasks, rinsed with a calcium- and magnesium-free salt solution and gently rocked for ~30 seconds. Thereafter, the solution was replaced with a cell dissociation solution consisting of phosphate buffered saline (PBS), EDTA, glycerol, and sodium citrate (from Sigma). This solution contains no protein and allows dislodging of cells without the use of enzymes. The cells were incubated in this solution for 5–10 min at 37°C and harvested by pipetting [23].

### 2.4. Determination of variation in membrane potential

Variation in cell membrane potential was determined with the use of DiS-C3-(5) according to established methods [23,24]. Briefly, the fluorescence of 1 μM DiS-C3-(5) was monitored at excitation and emission wavelengths of 620 and 660 nm, respectively in low or high K<sup>+</sup> solution (Solutions B and C, Table 1) in the absence of cultured cells. The mIMCD-3 cells in suspension were then added to the solution and the quenching of the fluorescence was determined within 30 sec. To demonstrate the validity of this approach, a suspension of cultured mIMCD-3 cells was incubated in high K<sup>+</sup> media to achieve a K<sup>+</sup>-loaded state (Solution C, Table 1). The K<sup>+</sup>-loaded cells were then diluted into a low K<sup>+</sup> solution (Solution B, Table 1) in the presence of DiS-C3-(5). Thereafter, 5 μM valinomycin was added to the cuvette and the extracellular [K<sup>+</sup>] was incrementally increased using aliquots of 3 M KCl (see Section 3). The validity of measurement of membrane potential variation by this method in renal cells has previously been established [18,23–26].

### 2.5. Materials

F-12/DME medium was purchased from GIBCO-BRL. DiS-C3-(5), BCECF, and nigericin were from Molecular Probes. Valinomycin and quinidine were from Fluka Chemika-Biochemika Analytika.

Amiloride, barium, DIDS, bumetanide, ouabain, and verapamil were purchased from Sigma Chemical Co. Schering 28080 was a generous gift from Schering Corp (via Dr. Cuppoletti, University of Cincinnati, USA).

## 2.6. Statistics

Results are expressed as means  $\pm$  S.E. Statistical significance between experimental groups was assessed by Student's *t* test or by one-way analysis of variance.

## 3. Results

### 3.1. Ammonium transport in mIMCD-3 cells

To examine whether  $\text{NH}_4^+$  enters the mIMCD-3 cells via a carrier-mediated process, cells were grown to confluence on coverslips and monitored for  $\text{pH}_i$  changes in NaCl solution (solution A, Table 1) or upon exposure to  $\text{NH}_4^+$ -containing solution (20 mM NaCl was replaced with 20 mM  $\text{NH}_4\text{Cl}$ ). Addition of 20 mM  $\text{NH}_4^+$  induced a rapid initial cell alkalinization, likely due to  $\text{NH}_3$  diffusion (Fig. 1a). Following this initial alkalinization,  $\text{pH}_i$  decreased to baseline in approx. 10 min. To determine whether this acidification represented  $\text{NH}_4^+$  entry, cells were alkalinized to the same level using sodium acetate or sodium propionate withdrawal [13] and monitored for  $\text{pH}_i$  recovery. As shown in Fig. 1a, except for a small drop, the cell pH did not recover from the initial cell alkalinization during the 10 min of  $\text{pH}_i$  monitoring. The rate of cell acidification was significantly higher in the presence of  $\text{NH}_4^+$  compared to acetate or propionate withdrawal ( $0.056 \pm 0.003$  for  $\text{NH}_4^+$  vs 0.009

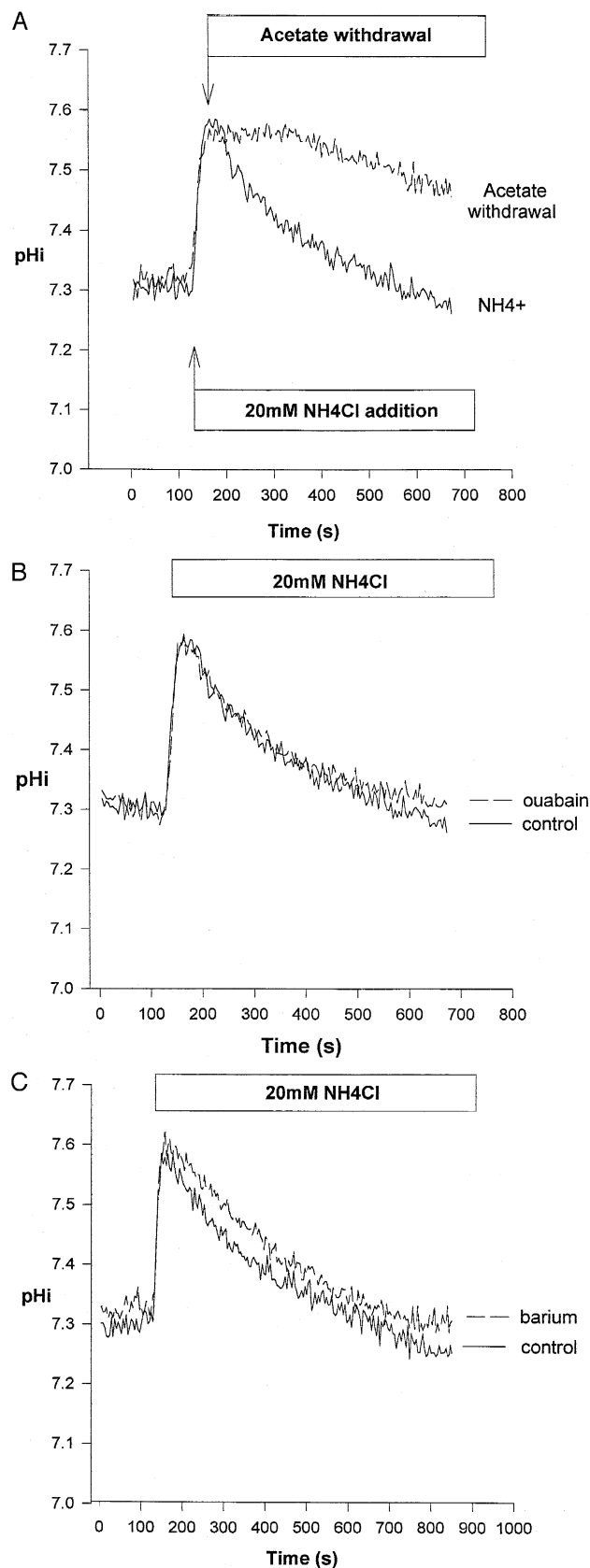


Fig. 1.  $\text{NH}_4^+$  transport in mIMCD-3 cells. (a) mIMCD-3 cells were alkalinized by preincubation and withdrawal of 20 mM acetate ( $n = 5$ ) or were exposed to 20 mM  $\text{NH}_4\text{Cl}$  ( $n = 5$ ). (b and c) Representative tracings showing exposure of mIMCD-3 cells to 20 mM  $\text{NH}_4\text{Cl}$  in the presence of 1 mM ouabain ((b),  $n = 6$ ) or 10 mM  $\text{BaCl}_2$  ((c),  $n = 5$ ) as compared to control (no inhibitor). Barium experiments were performed in phosphate-free solution (solution D, Table 1) in order to prevent Ba-phosphate precipitation. All inhibitors or their vehicles were added to the cells 2 min before  $\text{NH}_4^+$  addition.

$\pm 0.002$  for acetate withdrawal,  $P < 0.0001$ , and  $0.007 \pm 0.002$  pH/min for propionate withdrawal,  $P < 0.0001$ ). There was no difference in peak  $\text{pH}_i$  values achieved in  $\text{NH}_4\text{Cl}$  addition ( $7.567 \pm 0.008$ ) and acetate ( $7.557 \pm 0.009$ ,  $P > 0.4$ ; Fig. 1a) or propionate ( $7.549 \pm 0.011$ ,  $P > 0.2$ ;  $n = 4$ , data not shown) withdrawal. These results indicate that recovery

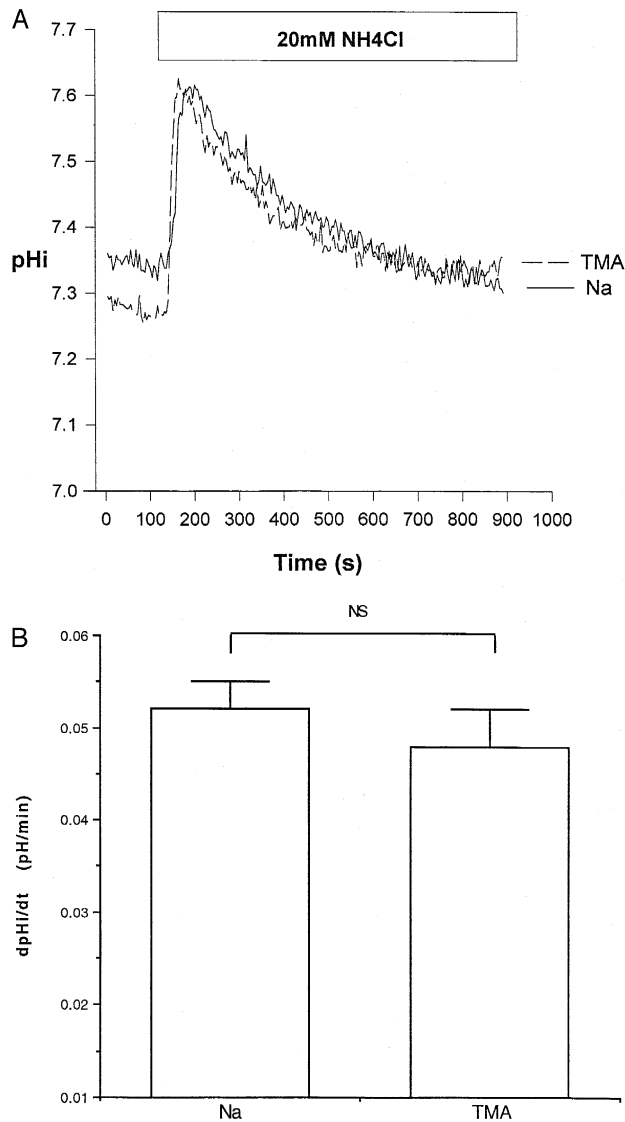


Fig. 2. Effect of  $\text{Na}^+$  on  $\text{NH}_4^+$  transport. mIMCD-3 cells were incubated in  $\text{Na}^+$ -containing (solution A, Table 1) or  $\text{Na}^+$ -free solution (solution B, Table 1) and assayed for  $\text{NH}_4^+$  transport. a. Representative tracing demonstrating  $\text{NH}_4^+$  transport in the presence or absence of sodium. Each datum (b) represents the mean  $\pm$  S.E. for the initial rate of  $\text{NH}_4^+$ -induced cell acidification ( $\text{dpH}_i/\text{dt}$ ) of indicated  $n$  runs.

Table 2

Effect of amiloride, barium, bumetanide, DIDS, and ouabain, on  $\text{dpH}_i/\text{dt}$  induced by  $\text{NH}_4^+$  entry into the cells

Groups	(n)	$\text{dpH}_i/\text{dt}$ (pH U/min)	P
Vehicle	5	$0.047 \pm 0.006$	
Amiloride	5	$0.049 \pm 0.007$	NS
Control	4	$0.049 \pm 0.005$	
Barium	5	$0.042 \pm 0.003$	NS
Vehicle	4	$0.048 \pm 0.004$	
Bumetanide	6	$0.045 \pm 0.002$	NS
Vehicle	4	$0.050 \pm 0.006$	
DIDS	5	$0.047 \pm 0.003$	NS
Vehicle	4	$0.054 \pm 0.003$	
Ouabain	6	$0.060 \pm 0.004$	NS

Values are mean  $\pm$  SE;  $n$ , number of coverslip;  $\text{dpH}_i/\text{dt}$ , the rate of cells acidification induced by  $\text{NH}_4^+$  entry into the cells. mIMCD-3 cells were incubated in  $\text{Na}^+$ -containing solution (Solution A, Table 1), in the absence (vehicle, DMSO) or presence of 500  $\mu\text{M}$  amiloride, 500  $\mu\text{M}$  bumetanide, 100  $\mu\text{M}$  DIDS (4,4'-di-isothiocyanostilbene-2-2'-disulfonic acid) or 1 mM ouabain 2 min. before  $\text{NH}_4\text{Cl}$  addition. 10 mM barium ( $\text{BaCl}_2$ ) was added isoosmotically to the solution A (15 mM  $\text{NaCl}$  replaced with 10 mM  $\text{BaCl}_2$ ), in the absence of phosphate ( $\text{KHPO}_4$  replaced with 1.8 mM  $\text{KCl}$ ).

ery from alkaline  $\text{pH}_i$  in the presence of  $\text{NH}_4^+$  in mIMCD-3 cells is due to  $\text{NH}_4^+$  entry.

### 3.2. Mechanism of $\text{NH}_4^+$ transport in mIMCD-3 cells

The mIMCD-3 cells express a  $\text{Ba}^{++}$ -sensitive  $\text{K}^+$  channel and an amiloride-sensitive  $\text{Na}^+$  channel [20] on their apical membranes, and a ouabain-sensitive  $\text{Na}^+\text{-K}^+\text{ATPase}$ , a furosemide-sensitive  $\text{Na}^+\text{-K}^+\text{-}2\text{Cl}^-$  cotransporters [27] and two isoforms of  $\text{Na}^+/\text{H}^+$  exchanger (NHE-1 and NHE-2) on their basolateral membranes [19]. Since  $\text{NH}_4^+$  has been shown to be transported via these pathways in other tissues [1,7–12], we sought to determine whether  $\text{NH}_4^+$  entry into mIMCD-3 cells was mediated by any of these transporters.

Cells were incubated in  $\text{Na}$ -containing media (solution A, Table 1) and then exposed to 20 mM  $\text{NH}_4\text{Cl}$  in the presence of ouabain at 1 mM (Fig. 1b) or barium at 10 mM (Fig. 1c). In addition to ouabain and barium, the effect of amiloride, 500  $\mu\text{M}$ , bumetanide, 500  $\mu\text{M}$ , or DIDS, 100  $\mu\text{M}$ , on  $\text{NH}_4^+$  transport was also tested. The summary of the results is included in Table 2 and shows that none of these

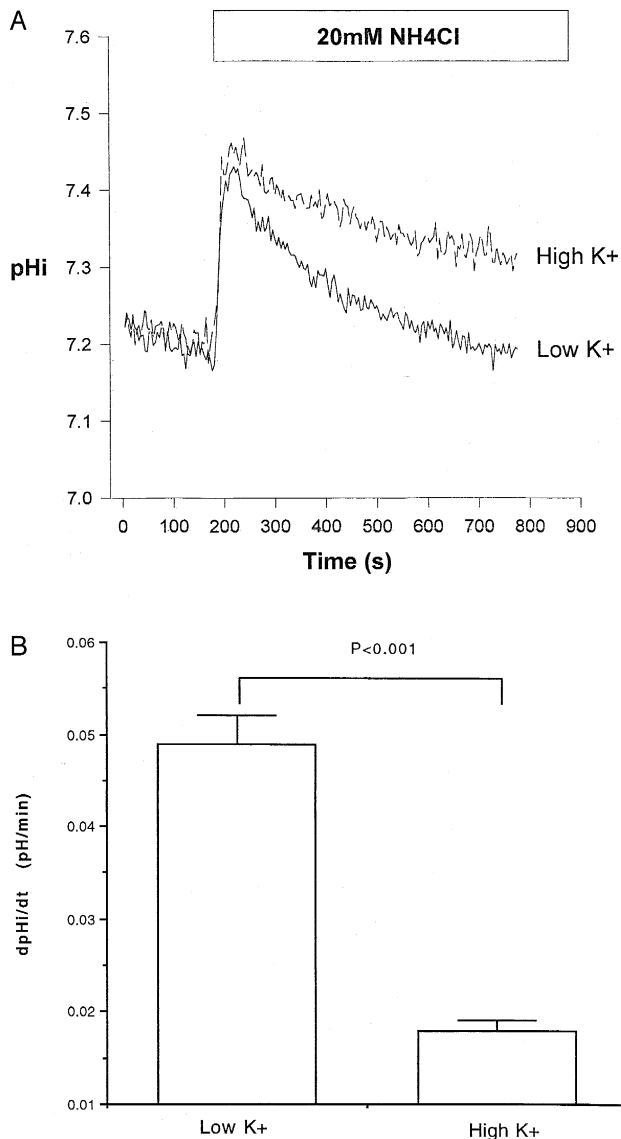


Fig. 3. Effect of high and low  $K^+$  on  $NH_4^+$  transport. Cells were incubated in  $Na^+$ -free solution in the presence of low or high  $K^+$  (solutions B and C, Table 1) and assayed for  $NH_4^+$  transport. a. Representative tracing demonstrating  $NH_4^+$  transport in the presence of high or low  $K^+$ . Each datum (b) represents the mean  $\pm$  S.E. for the initial rate of  $NH_4^+$ -induced cell acidification ( $dpH_i/dt$ ) of indicated  $n$  runs for high or low  $K^+$ .

inhibitors altered  $pH_i$  recovery as determined by  $dpH_i/dt$ . These results indicate that the corresponding transporters for these inhibitors ( $Na^+K^+$ -ATPase,  $K^+$  channel,  $Na^+/H^+$  exchange or sodium channel,  $Na^+K^+2Cl^-$  cotransport, and  $Cl^-$ /base exchange) do not mediate the transport of  $NH_4^+$  in mIMCD-3

cells. In additional experiments, we found that presence or absence of extracellular calcium had no effect on  $NH_4^+$  entry into mIMCD-3 cells ( $0.042 \pm 0.008$  in

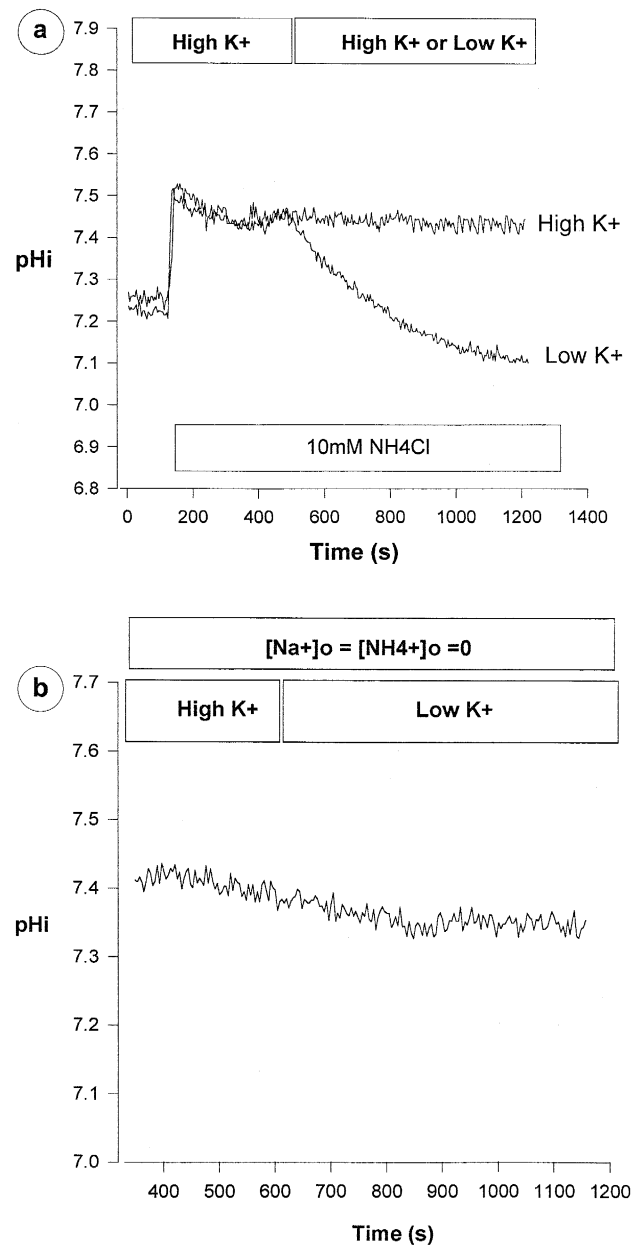


Fig. 4.  $K^+$  efflux-induced  $NH_4^+$ -dependent cell acidification. mIMCD-3 cells were incubated in a  $Na^+$ -free high  $K^+$  solution (solution C, Table 1) and then exposed to 10 mM  $NH_4Cl$ . At steady state ( $pH_i \sim 7.40$ ), cells were perfused with either the same solution or switched to a  $Na^+$ -free low  $K^+$  solution that contained 10 mM  $NH_4Cl$ . Representative tracings show the effect of an outward  $K^+$  gradient imposition on cell pH as compared to no outward  $K^+$  gradient in the presence (a) or absence of  $NH_4^+$  (b).

the presence and  $0.039 \pm 0.003$  pH/min in the absence of  $\text{Ca}^{2+}$ ,  $P > 0.05$ ).

To determine whether  $\text{NH}_4^+$  transport in mIMCD-3 cells occurs via a Na-dependent pathway, NaCl was replaced with equimolar concentration of TMACl (tetramethylammonium chloride) (solution B, Table 1). Fig. 2a shows representative  $\text{pH}_i$  tracings of  $\text{NH}_4^+$  entry in mIMCD-3 cells in the presence or absence of sodium. As further shown in Fig. 2b, the rate of  $\text{NH}_4^+$  entry ( $\text{NH}_4^+$ -induced cell acidification) was not altered in the presence of sodium in the media ( $0.052 \pm 0.003$  in the presence of  $\text{Na}^+$  vs  $0.048 \pm 0.004$  pH/min in the absence of  $\text{Na}^+$ ,  $P > 0.05$ ), indicating that the transport of  $\text{NH}_4^+$  into mIMCD-3 cells was sodium independent. The rest of the experiments (Figs. 3–9) were performed in Na-free solution.

### 3.3. Interaction of external $\text{K}^+$ with $\text{NH}_4^+$ transport

It has been shown that the hydrated radius of  $\text{NH}_4^+$  is very similar to that of  $\text{K}^+$  and, therefore, may compete with  $\text{K}^+$  for the same binding site [4]. To determine whether  $\text{NH}_4^+$  transport in mIMCD-3 cells interacts with  $\text{K}^+$ , cells were incubated in the presence of low  $\text{K}^+$  or high  $\text{K}^+$  solution (Table 1, solutions B and C) and monitored for  $\text{pH}_i$  changes upon exposure to ammonium (20 mM TMA-Cl or KCl was replaced with 20 mM  $\text{NH}_4\text{Cl}$ ). Representative  $\text{pH}_i$  tracings (Fig. 3a) demonstrate that  $\text{NH}_4^+$

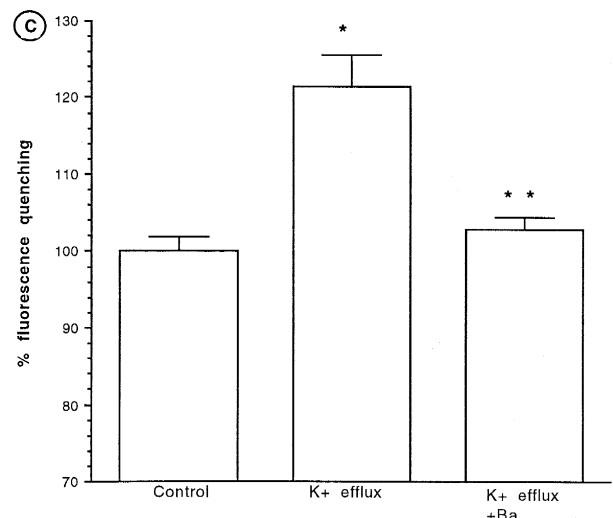
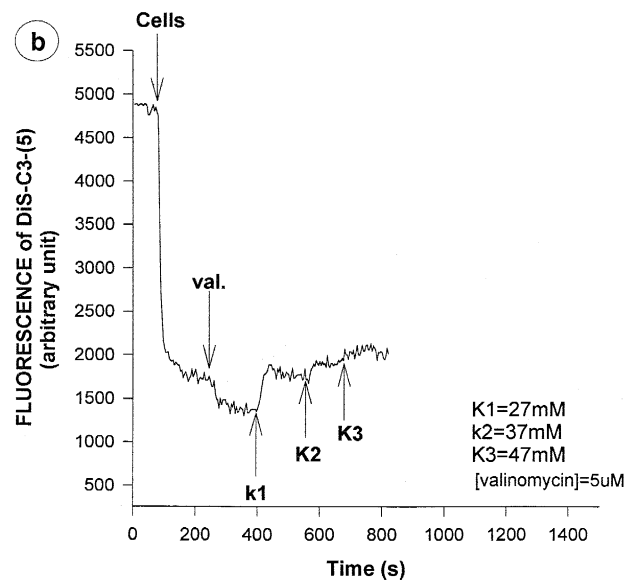
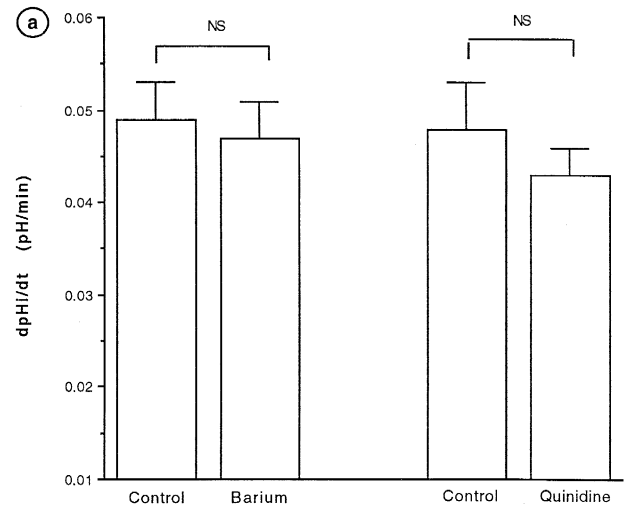
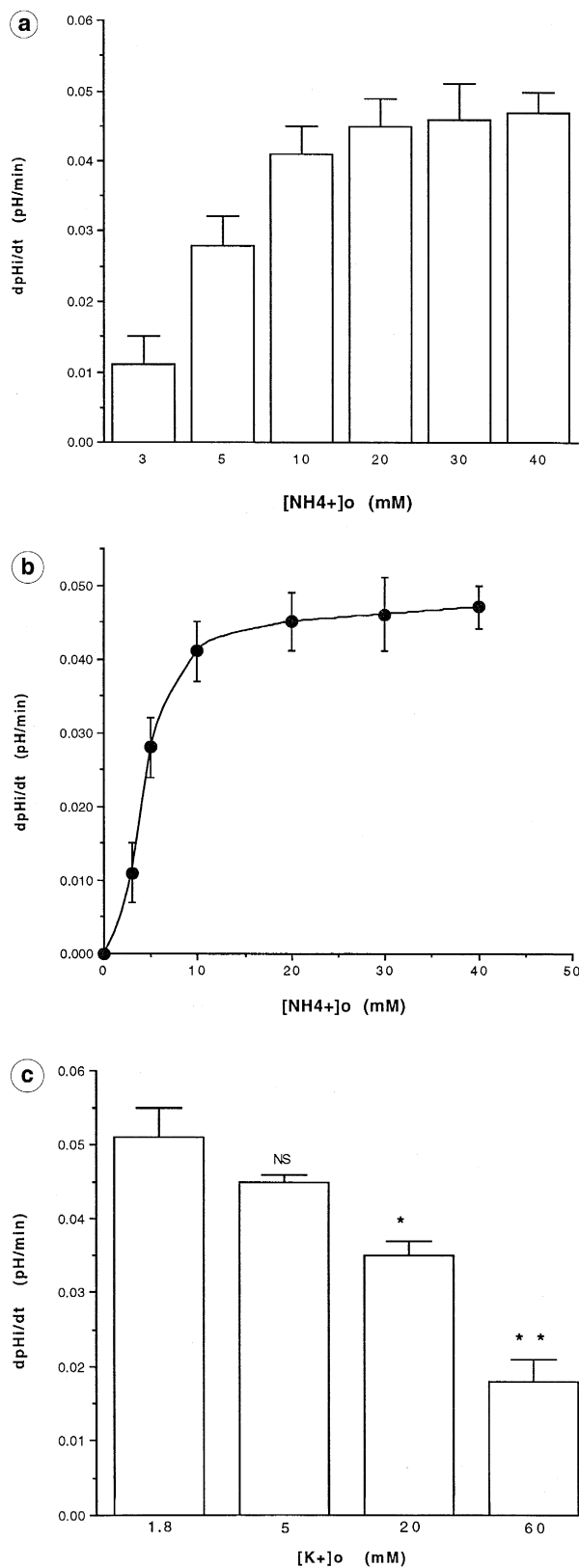


Fig. 5. Electroneutrality of  $\text{K}^+$  efflux-induced  $\text{NH}_4^+$  entry. a. mIMCD-3 cells were incubated in a  $\text{Na}^+$ -free high  $\text{K}^+$  solution (solution C, Table 1) and then exposed to 10 mM  $\text{NH}_4\text{Cl}$ . Thereafter, and at a steady-state condition ( $\text{pH}_i \sim 7.40$ ), cells were switched to a  $\text{Na}^+$ -free low  $\text{K}^+$  solution that contained 10 mM  $\text{NH}_4\text{Cl} \pm 10$  mM barium or  $\pm 500$   $\mu\text{M}$  quinidine. Each datum represents mean  $\pm$  S.E. for 5 separate experiments. b. mIMCD-3 cell suspensions were preincubated in a  $\text{Na}^+$ -free high  $\text{K}^+$  solution and were added to a  $\text{Na}^+$ -free low  $\text{K}^+$  solution that contained 2  $\mu\text{M}$  of DiS-C3-(5). The fluorescence of the probe was quenched. Thereafter, valinomycin (val.) was added and  $\text{K}^+$  concentration was incrementally increased to 27, 37, and 47 mM using aliquots from a 3 M KCl stock solution ((b) is a representative reproduction of 4 experiments). c. The quench of DiS-C3-(5) probe was determined after cells were added into the same media (high  $\text{K}^+$ ; control,  $n = 7$ ) or into a low  $\text{K}^+$  medium in the absence ( $\text{K}^+$  efflux,  $n = 6$ ) or in the presence of 10 mM  $\text{BaCl}_2$  ( $\text{K}^+$  efflux + Ba,  $n = 5$ ). \*  $P < 0.004$  compared to control; \*\*  $P < 0.01$  compared to  $\text{K}^+$  efflux + Ba.



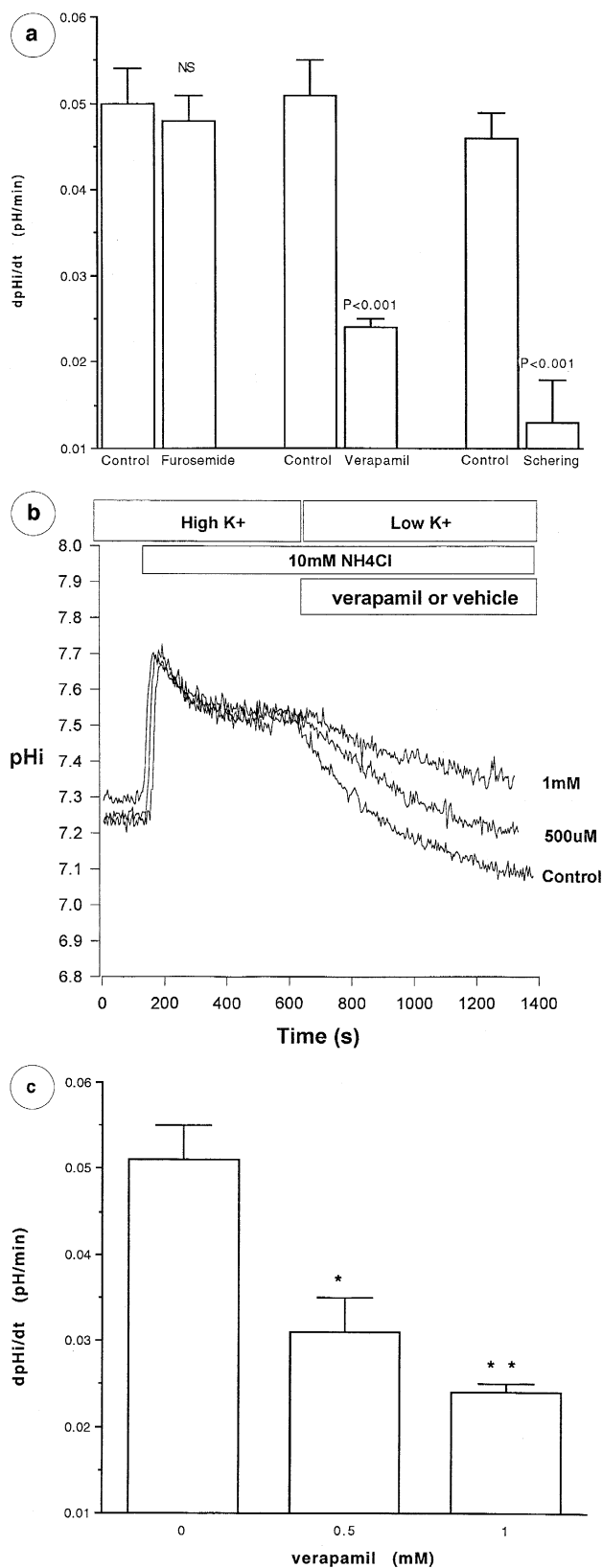
entry into mIMCD-3 cells was significantly blocked in high  $\text{K}^+$  solution. The results of five separate experiments (Fig. 3b) showed that the rate of  $\text{NH}_4^+$ -induced cell acidification was significantly lower in high  $\text{K}^+$  media vs low  $\text{K}^+$  media ( $0.049 \pm 0.003$  vs  $0.018 \pm 0.001$  pH/min for 1.8 mM  $\text{K}^+$  vs 120 mM  $\text{K}^+$  in the media, respectively,  $P < 0.001$ ). The baseline  $\text{pH}_i$  before and the peak  $\text{pH}_i$  following exposure to  $\text{NH}_4^+$  were not different between the two groups.

### 3.4. $\text{K}^+$ efflux-induced $\text{NH}_4^+$ entry

The studies shown in Fig. 3 were performed in cells incubated in high or low  $\text{K}^+$  solution for the entire duration of the experiments. To gain insight into the mechanism of interaction of  $\text{K}^+$  with  $\text{NH}_4^+$ , the  $\text{NH}_4^+$  transport into mIMCD-3 cells was studied upon imposition of an outward  $\text{K}^+$  gradient. The purpose of this approach was to study the effect of  $\text{K}^+$  efflux on  $\text{NH}_4^+$  entry. Accordingly, cells were incubated in the presence of high  $\text{K}^+$  (solution C, Table 1), exposed to ammonium (10 mM KCl was replaced with 10 mM  $\text{NH}_4\text{Cl}$ ), and monitored for  $\text{pH}_i$  changes (the experiments were performed in the presence of 10 mM  $\text{NH}_4\text{Cl}$ , as K-dependent  $\text{NH}_4^+$  entry is saturated at this concentration of  $\text{NH}_4^+$ , see Fig. 6 on kinetic analysis of this transporter). Following initial cell alkalinization and reaching steady-state  $\text{pH}_i$ , an outward  $\text{K}^+$  gradient was imposed across the cells by changing to a low  $\text{K}^+$ -containing solution with 10 mM  $\text{NH}_4^+$  (10 mM TMA-Cl of solution B was replaced with 10 mM  $\text{NH}_4\text{Cl}$ ). As shown in Fig. 4a, imposing an outward  $\text{K}^+$  gradient acutely acidified the cells. The results of five separate experiments showed that imposing an outward  $\text{K}^+$  gradient resulted in  $0.264 \pm 0.032$  pH units acidification in 10 min. This acidification was only observed in the

Fig. 6. Kinetic analysis of  $\text{K}^+/\text{NH}_4^+$  antiport. Initial rate of  $\text{K}^+$  efflux-induced  $\text{NH}_4^+$  entry ( $\text{dpH}_i/\text{dt}$ ) was measured in the presence of varying concentrations of  $\text{NH}_4^+$  (a). Michaelis-Menten replot of the data shows a  $K_m$  of  $\sim 5$  mM for  $\text{NH}_4^+$  (b). Inhibitory concentration ( $K_{1/2}$ ) of external  $\text{K}^+$  on  $\text{K}^+/\text{NH}_4^+$  antiport at constant  $\text{NH}_4^+$  concentration is shown in (c). Each datum represents mean  $\pm$  S.E. for 5 separate experiments; \*  $P < 0.003$  compared to 1.8 mM  $\text{K}^+$ ; \*\*  $P < 0.001$  compared to 20 mM  $\text{K}^+$ .





presence of  $NH_4^+$ , as imposing an outward  $K^+$  gradient in the absence of  $NH_4^+$  but in the presence of comparable alkaline  $pH_i$  (using acetate withdrawal method) did not induce any significant cell acidification (representative tracing in Fig. 4b).

### 3.5. Electroneutrality of $K^+$ efflux-induced $NH_4^+$ entry

Alterations in extracellular  $K^+$  could affect the magnitude of membrane potential. Conceivably, acute  $NH_4^+$ -induced cell acidification that was observed in the presence of an outward  $K^+$  gradient could be due to membrane hyperpolarization. To address this issue, the effect of two known  $K^+$  channel inhibitors (barium and quinidine) on  $K^+$  efflux-coupled  $NH_4^+$  entry was examined. Fig. 5a demonstrates that addition of 10 mM barium or 500  $\mu$ M quinidine to low  $K^+$  solutions did not inhibit the  $NH_4^+$ -dependent  $K^+$  efflux-induced cell acidification. To determine whether 10 mM barium could inhibit the cell membrane hyperpolarization induced by  $K^+$  efflux, variations in membrane potential were measured by the use of DiS-C3-(5) probe as described in Section 2. Fig. 5b is a representative tracing demonstrating sensitivity of DiS-C3-(5) to membrane potential variation and shows that imposing an outward  $K^+$  gradient causes significant quenching in DiS-C3-(5) fluorescence. Addition of valinomycin causes further quenching due to cell membrane hyperpolarization caused by further efflux of  $K^+$  via the ionophore. Increasing the extracellular  $K^+$  concentration gradually increased the fluorescence due to progressive membrane depolarization and, as a result, exit of the dye from the cells. These observation indicate the sensitivity of DiS-C3-(5) probe to membrane poten-

Fig. 7. Inhibition of  $K^+/NH_4^+$  antiport by verapamil. mIMCD-3 cells were incubated in  $Na^+$ -free high  $K^+$  medium and then exposed to 10 mM  $NH_4Cl$ . At steady-state  $pH_i$ , cells were perfused with  $Na^+$ -free low  $K^+$  media in the absence or presence of 1.5 mM furosemide, 1 mM verapamil, or 300  $\mu$ M Schering 28080 (a). b. Representative  $pH_i$  tracings of  $NH_4^+$  transport inhibition at 0.5 and 1 mM verapamil. c. Each datum represents mean  $\pm$  S.E. for control ( $n = 12$ ), 0.5 mM verapamil ( $n = 5$ ; \*  $P < 0.02$  compared to control), or 1 mM verapamil ( $n = 5$ ; \*\*  $P < 0.001$  compared to control).

tial variations. To determine whether barium blocked membrane hyperpolarization resulting from an outward imposition of  $K^+$  gradient, the experiments were performed in the presence or absence of barium in the solution. As shown in Fig. 5c, imposing an outward  $K^+$  gradient (middle bar) significantly increased quenching of the probe as compared to no outward  $K^+$  gradient (left bar), consistent with membrane hyperpolarization. The presence of 10 mM barium completely blocked  $K^+$ -efflux induced membrane hyperpolarization (right bar). Presence or absence of  $NH_4^+$  had no effect on membrane potential variation. Thus, the  $K^+$  efflux-induced  $NH_4^+$ -dependent cell acidification occurred both with membrane hyperpolarisation (concomitant  $K^+$  efflux through  $K^+$  channel) and no change in the cell PD ( $K^+$  channel blockade by barium). These results indicate that  $K^+$ -efflux induced  $NH_4^+$  entry into mIMCD-3 cells is not mediated via alterations in membrane potential, and further, that this transporter is likely an

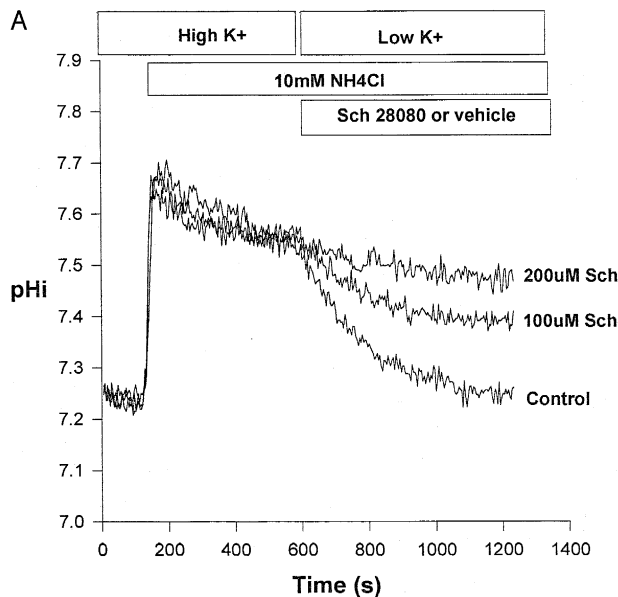


Fig. 8. Inhibition of  $K^+/NH_4^+$  antiport by Schering 28080. mIMCD-3 cells incubated in  $Na^+$ -free high  $K^+$  medium were exposed to 10 mM  $NH_4Cl$ . Following the initial cell alkalinization, the cells were perfused with  $Na^+$ -free low  $K^+$  solution in the presence of 10 mM  $NH_4Cl \pm$  Schering 28080. a. Representative  $pH_i$  tracings in the absence or in the presence of various concentrations of Sch28080. b. Each datum represents mean  $\pm$  S.E. for 4–7 separate experiments. Inset: Dixon plot of data ( $r = 0.994$ ).

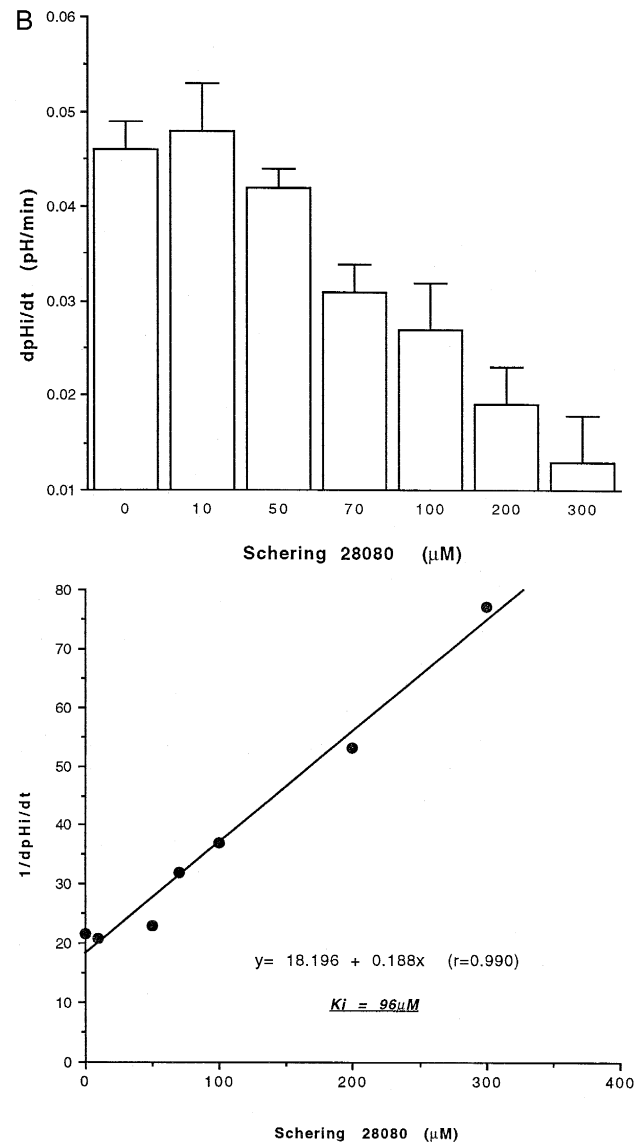


Fig. 8 (continued).

electroneutral process. To study the properties of this transporter further, the rest of the experiments were performed using the  $K^+$  efflux-coupled  $NH_4^+$  entry protocol as described in Fig. 4a.

### 3.6. Kinetic analysis of $K^+-NH_4^+$ antiport

The results of the above experiments indicate that  $NH_4^+$  transport in mIMCD-3 cells is independent of sodium, is coupled to  $K^+$  efflux, is not mediated via  $K^+$  channels, and is competitively inhibited by exter-

nal  $K^+$ . These results are consistent with an  $NH_4^+/K^+$  antiport. Such a transporter could exchange extracellular  $NH_4^+$  with intracellular  $K^+$  and mediate the transport of  $NH_4^+$  in mIMCD-3 cells. In the next series of experiments, the kinetics of the  $K^+/NH_4^+$  antiporter were studied. To determine the relative affinity of  $NH_4^+$  for the  $K^+/NH_4^+$  antiporter, the rate of cell acidification was monitored in the presence of an increasing concentration of  $NH_4^+$  at constant outward potassium gradient.  $NH_4^+$ -induced cell acidification was a saturable process with respect to  $NH_4^+$  concentration (Fig. 6a): the  $K_m$  for  $NH_4^+$  was  $\sim 5$  mM (Fig. 6b).

The purpose of the next series of experiments was to study the interaction of external  $K^+$  with  $NH_4^+$  transport. Cells were incubated in high  $K^+$  solution (solution C, Table 1) and were then exposed to 10 mM  $NH_4Cl$  and allowed to reach steady state  $pH_i$ . Thereafter, cells were switched to solutions with varying  $K^+$  concentration (1.8 to 60 mM) at constant  $NH_4^+$  concentration. As shown in Fig. 6c, external  $K^+$  inhibits  $NH_4^+$  transport in a concentration dependent manner.

### 3.7. Inhibitory profile of $K^+/NH_4^+$ antiport

$K^+/NH_4^+$  antiport was not inhibited by ouabain, amiloride, quinidine, bumetanide, and barium (Figs. 1 and 5 and Table 2). To examine the inhibitory profile of  $K^+/NH_4^+$  antiport further, the effect of a variety of inhibitors was tested. Fig. 7a shows the effect of 1.5 mM furosemide, 1 mM verapamil, and 300  $\mu$ M Schering 28080 on  $K$ -dependent  $NH_4^+$  transport. The results indicated that two inhibitors amongst all chemicals tested, verapamil and Schering 28080, inhibited  $K^+/NH_4^+$  antiport. Shown in Fig. 7b are  $pH_i$  tracings monitoring  $K^+$  efflux-induced  $NH_4^+$  entry in the presence of 0.5 and 1 mM verapamil compared to no inhibitor. The results of these tracings and five separate coverslips (Fig. 7c) indicate that verapamil significantly inhibited  $K^+/NH_4^+$  antiporter. The inhibitory effect of Schering 28080 on  $K^+/NH_4^+$  antiport was next tested. Fig. 8a illustrates tracings of Schering 28080-induced inhibition of  $NH_4^+$ -induced  $pH_i$  alterations in mIMCD-3 cells. Shown in Fig. 8b is dose response inhibition of the effect of Schering 28080 on  $dpH_i/dt$ . The Dixon plot of the  $dpH_i/dt$

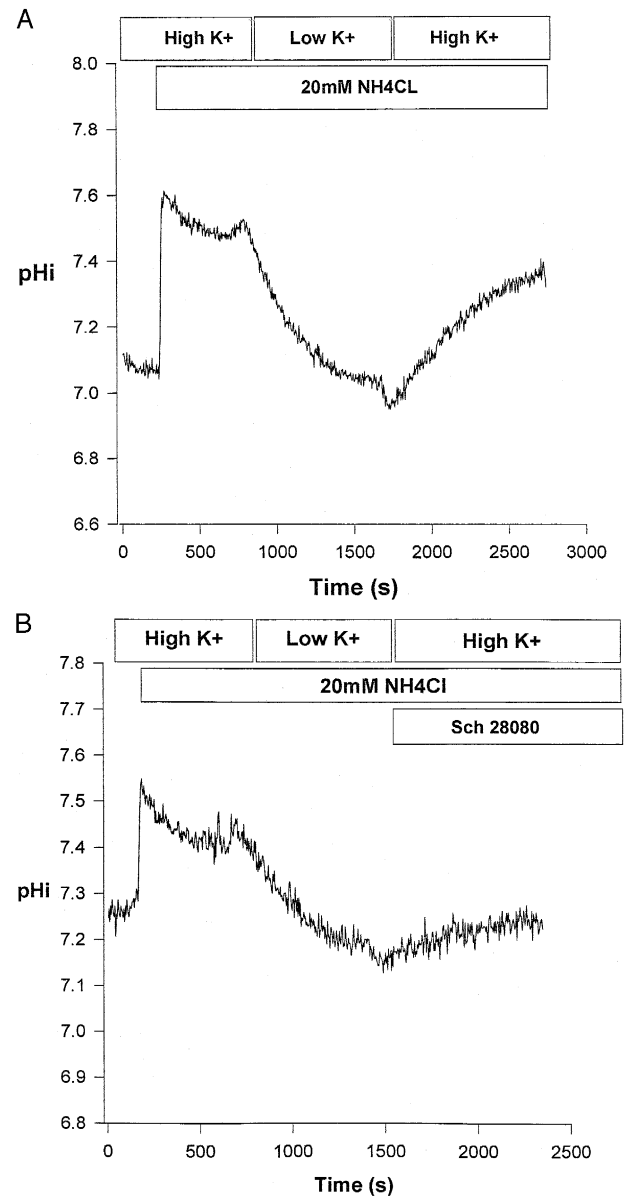


Fig. 9. Modes of  $K^+/NH_4^+$  antiport function. mIMCD-3 cells loaded with  $NH_4^+$  (20 mM  $NH_4Cl$ ) were allowed to reach steady  $pH_i$  in low  $K^+$  solution. Thereafter, cells were switched to a high  $K^+$  solution in the presence of 20 mM  $NH_4Cl$ . a. Representative  $pH_i$  tracing showing cell alkalinization upon imposition of an inwardly directed  $K^+$  gradient. b. Shows that high  $K^+$ -induced  $NH_4^+$  efflux was abolished by 200  $\mu$ M Sch28080.

values yielded a straight line consistent with a single Sch28080 site having an apparent inhibitory constant ( $K_i$ ) of 96  $\mu$ M (Fig. 8b, inset).

### 3.8. Modes of $K^+/NH_4^+$ antiport operation

To determine whether  $K^+/NH_4^+$  antiport can operate in a reverse mode, cells were incubated with  $NH_4^+$  in the presence of an outward  $K^+$  gradient for 15 min in a manner similar to previous figures. The cell acidification following the initial alkalization was complete at 15 min as shown by  $pH_i$  tracing, indicating presence of equilibrium state and therefore  $NH_4^+$  loading of the cells (Fig. 9a). The cells were then switched to a high  $K^+$  solution (solution C). Exposure of  $NH_4^+$ -loaded cells to  $NH_4^+$ -containing high  $K^+$  solution resulted in rapid cell alkalization (Fig. 9a). The results of 4 separate experiments showed that switching  $NH_4^+$ -loaded cells from low (1.8 mM) to high (130 mM)  $K^+$  increased the  $pH_i$  by  $0.36 \pm 0.09$  pH unit,  $P < 0.01$  (Fig. 9a). In the presence of Schering 28080, 200  $\mu$ M,  $K^+$ -induced cell alkalization was blocked (Fig. 9b). Switching mIMCD-3 cells from low to high  $K^+$  solution in the absence of  $NH_4^+$  had no effect on steady state  $pH_i$  ( $n = 5$ , data not shown). The results of the above experiments are consistent with  $K^+$ -induced  $NH_4^+$  efflux, indicating that the  $K^+/NH_4^+$  antiport can function in a reverse direction.

## 4. Discussion

$NH_4^+$  excretion is the major mechanism by which the body eliminates the increased metabolic acid load and therefore is essential for maintenance of acid base balance [1]. It has been shown that decreased  $NH_4^+$  excretion impairs the ability of the body to eliminate metabolically-generated acid load and conversely, increased  $NH_4^+$  excretion enables the body to get rid of the increased acid load [1,4–6]. Ammonium is synthesized in the mitochondria of proximal tubule cells by deamination of glutamine, transported to the cytosol and excreted in part via the  $Na^+/H^+$  exchanger [7,8]. Once in the lumen of proximal tubule, it is delivered to medullary thick ascending limb of Henle where it is reabsorbed via a number of transport pathways [9–12,17]. The reabsorbed  $NH_4^+$  enters the interstitium, is transported to the medullary collecting duct cells, and secreted into the collecting duct lumen [1,4–6]. The mechanism of  $NH_4^+$  trans-

port in the medullary collecting duct is poorly understood [1].

Present studies suggest that  $NH_4^+$  entry in mouse cultured inner medullary collecting duct (mIMCD-3) cells is carrier-mediated.  $NH_4^+$  entry occurs via a  $K^+$ -dependent pathway that was distinct from  $Na^+$ - $K^+$ -ATPase,  $Na^+$ - $K^+$ -2Cl $^-$ ,  $K^+/H^+$  antiport, or  $K^+$ -channel (Figs. 1 and 2 and Table 2). Imposing an outward  $K^+$  gradient ( $K^+$  efflux) was coupled to enhanced  $NH_4^+$  entry into mIMCD-3 cells (Fig. 4). Coupling of  $K^+$  efflux to  $NH_4^+$  entry was not affected by alterations in membrane potential (Fig. 5). Indeed, 10 mM barium or 500  $\mu$ M quinidine which blocks potassium channels had no effect on  $NH_4^+$  transport (Fig. 5). The results further demonstrated that  $NH_4^+$  transport was not driven by secondary alterations in membrane potential, but rather was mediated by an electroneutral transport process (Fig. 5c). Taken together, these results are consistent with the presence of  $K^+/NH_4^+$  antiport in mIMCD-3 cells. The  $K^+/NH_4^+$  antiporter did not show any affinity for  $H^+$  (Fig. 4), thus, making it distinct from the  $K^+/H^+/NH_4^+$  transporter [18].

The results of the experiments in Figs. 1–3 show that absence of sodium or presence of bumetanide did not affect  $NH_4^+$  transport, indicating that  $Na^+:K^+:2Cl^-$  does not contribute to  $NH_4^+$  transport in mIMCD-3 cells. These results are interesting since studies in mTAL cells have shown that  $NH_4^+$  absorption occurs predominantly via the  $Na^+:K^+:2Cl^-$  cotransporter [9–12]. While mIMCD-3 cells express a  $Na^+:K^+:2Cl^-$  cotransporter, the structure of that gene [27] is distinct from the luminal mTAL  $Na^+:K^+:2Cl^-$  cotransporter [28]. Moreover, the basolateral membrane localization of  $Na^+:K^+:2Cl^-$  cotransporter in mIMCD-3 cells [27] suggest that these two isoforms perform different functions. Amiloride, an inhibitor of  $Na^+/H^+$  exchange or  $Na^+$  channel [29], did not block  $NH_4^+$  entry, indicating lack of involvement of these two transporters in mIMCD-3 cells. Recent studies in kidney proximal tubule have shown that  $Na^+/H^+$  exchange transports  $NH_4^+$  [7]. Lack of involvement of  $Na^+/H^+$  in mediating  $NH_4^+$  transport in mIMCD-3 cells may reflect either isoform difference (NHE-2 in mIMCD-3 cells vs NHE-3 in proximal tubule cells) or tissue specificity in this regard.

The role of  $Na^+:K^+$ -ATPase in  $NH_4^+$  transport has been controversial. Several recent reports have shown

no affinity of  $\text{Na}^+:\text{K}^+$ -ATPase for  $\text{NH}_4^+$  in kidney tubules and vascular smooth muscle cells [15,30,31]. However, two studies in microperfused rabbit proximal tubule [14] and rat medullary collecting duct [32] have shown that  $\text{Na}^+:\text{K}^+$ -ATPase can interact with  $\text{NH}_4^+$ . The interaction of  $\text{NH}_4^+$  with  $\text{Na}^+:\text{K}^+$ -ATPase in the latter studies [32] was demonstrated by inhibition by ouabain of  $\text{NH}_4\text{Cl}$ -induced increase in net acid secretion in rat IMCD at steady state. The results of those experiments are not in conflict with the current experiments. In the present experiments, we found that  $\text{Na}^+:\text{K}^+$ -ATPase did not contribute to  $\text{NH}_4^+$  transport in mIMCD-3 cells, as measured by initial entry of  $\text{NH}_4^+$  into mIMCD-3 cells. However, the contribution of  $\text{Na}^+:\text{K}^+$ -ATPase to the initial rate of  $\text{NH}_4^+$  transport was not studied in rat IMCD microperfusion experiments [32]. It is therefore likely that inhibition of  $\text{Na}^+:\text{K}^+$ -ATPase by ouabain, as employed in steady state net acid secretion measurements [32], could have depleted intracellular  $[\text{K}^+]$  and thus inhibited  $\text{K}^+/\text{NH}_4^+$  antiporter. In support of this view, we find that depletion of intracellular  $\text{K}^+$  by preincubation of mIMCD-3 cells in  $\text{K}^+$  and  $\text{Na}^+$ -free solution for 30 minutes inhibited  $\text{NH}_4^+$  entry into mIMCD-3 cells ( $0.053 \pm 0.004$  in normal K vs  $0.039 \pm 0.002$  pH/min in  $\text{K}^+$ -depleted cells,  $P < 0.02$ ). Another plausible explanation in this regard could be species specificity of  $\text{NH}_4^+$  affinity for  $\text{Na}^+:\text{K}^+$ -ATPase as those studies were performed in rat and rabbit [13,14,32]. Our results are consistent with the results of studies in kidney proximal tubule cells [15], cortical collecting duct cells [31], and vascular smooth muscle cells [30] indicating that  $\text{Na}^+:\text{K}^+$ -ATPase is not involved in  $\text{NH}_4^+$  transport.

The  $\text{K}^+/\text{NH}_4^+$  antiport that is described in the present studies is distinct from the  $\text{K}^+/\text{H}^+$  antiport in rat mTAL cells that carries  $\text{NH}_4^+$  [18] or  $\text{K}^+/\text{H}^+$  antiport that is identified in cultured opossum kidney (OK) cells [33]. The  $\text{K}^+/\text{NH}_4^+$  antiport has no affinity for  $\text{H}^+$  as shown in Fig. 4b demonstrating that in the absence of  $\text{NH}_4^+$ , induction of an outward  $\text{K}^+$  gradient had no effect on cell pH. We further find that in the absence of  $\text{NH}_4^+$ , increasing the extracellular potassium (from 1.8 to 140 mM) had no effect on  $\text{pH}_i$  (data not shown). In addition, the  $\text{K}^+/\text{NH}_4^+$  antiporter was not inhibited by barium (Fig. 1c, Fig. 5a and Table 2). Taken together, these results indicate that the  $\text{K}^+/\text{NH}_4^+$  antiporter is dis-

tinct from  $\text{K}^+/\text{H}^+$  antiport in mTAL cells (which has affinity for  $\text{NH}_4^+$ ) or from  $\text{K}^+/\text{H}^+$  antiport described in (OK) cells [18,33]. The  $\text{K}^+/\text{NH}_4^+$  antiport is also distinct from the  $\text{H}^+/\text{K}^+$ -ATPase described in various nephron segments [34–37]. While we have not examined the affinity of  $\text{NH}_4^+$  for the  $\text{K}^+$  binding site of  $\text{H}^+/\text{K}^+$ -ATPase, the results do not support a role for  $\text{H}^+/\text{K}^+$ -ATPase in  $\text{NH}_4^+$  transport in mIMCD-3 cells for the following reasons. First, a possible exchange of extracellular  $\text{NH}_4^+$  for intracellular  $\text{H}^+$  via  $\text{H}^+/\text{K}^+$ -ATPase should at best be neutral with respect to  $\text{pH}_i$ . However, the transport of  $\text{NH}_4^+$  in the current experiments (Figs. 1–9) causes cell acidification, indicating the exchange of  $\text{NH}_4^+$  with a non-acidic cation (i.e.  $\text{K}^+$  in this occasion). Moreover, the sensitivity of the  $\text{K}^+/\text{NH}_4^+$  antiport inhibition to Schering 28080 ( $\text{IC}_{50} \sim 96 \mu\text{M}$ ) is much less than the sensitivity of the  $\text{H}^+/\text{K}^+$ -ATPase to this inhibitor ( $\text{IC}_{50} < 10 \mu\text{M}$ ) reported in mIMCD-3 cells [37] and other investigations [34]. Lastly, the  $\text{K}^+$ -induced cell alkalization in mIMCD-3 cells loaded with  $\text{NH}_4^+$  (Fig. 9) indicates that this transporter exchanges  $\text{K}^+$  for  $\text{NH}_4^+$  and could function in a reverse mode, a feature not shared by  $\text{H}^+/\text{K}^+$ -ATPase.

The  $\text{K}^+/\text{Cl}^-$  cotransporter has been shown to accept  $\text{NH}_4^+$  in place of  $\text{K}^+$  in mTAL cells of rat kidney [12]. However, the  $\text{NH}_4^+$  transport in mIMCD-3 cells is not mediated via  $\text{K}^+/\text{Cl}^-$  cotransport, as barium (Fig. 5a) and furosemide (Fig. 7a), two strong inhibitors of  $\text{K}^+/\text{Cl}^-$  cotransport [12,38–40], had no effect on  $\text{NH}_4^+$  dependent cell acidification in mIMCD-3 cells. An amiloride-sensitive  $\text{NH}_4^+$  conductance and a nonspecific amiloride-sensitive cation channel in mTAL [18] and IMCD [41] cells have shown affinity for  $\text{NH}_4^+$ . However, the presence of amiloride had no effect on  $\text{NH}_4^+$  transport in mIMCD-3 cells, indicating lack of involvement of this channel (Table 2).

The kinetic analysis studies (Fig. 6c) demonstrate that increasing the  $\text{K}^+$  concentration from 5 to 20 mM significantly inhibited  $\text{NH}_4^+$  entrance in mIMCD-3 cells. These are relevant physiological concentrations with respect to  $\text{K}^+$  concentration in the interstitium of inner medulla [35,42] and indicate that increasing or decreasing the  $\text{K}^+$  concentration within the physiologic range could significantly affect  $\text{NH}_4^+$  entrance in mIMCD-3 cells and, as a

result, regulate acid secretion into the urine. If such were the case, hyperkalemic metabolic acidosis [43,44] may in part result from inhibition of  $\text{NH}_4^+$  entrance into the medullary collecting duct cells. Conversely, potassium depletion metabolic alkalosis [43,45,46] may, in part, result from enhanced  $\text{NH}_4^+$  entrance into the medullary collecting duct cells. The affinity of  $\text{NH}_4^+$  for  $\text{NH}_4^+$ -binding site of  $\text{K}^+/\text{NH}_4^+$  antiporter was found to be  $\sim 5$  mM (Fig. 6);  $\text{NH}_4^+$  concentration in the inner medulla is about  $\sim 10$  mM [5,6]. Thus, alterations in  $\text{NH}_4^+$  concentration within physiologic range could significantly affect the activity of  $\text{K}^+/\text{NH}_4^+$  antiporter and change the rate of  $\text{NH}_4^+$  entrance in mIMCD-3 cells. This in turn would alter the rate of luminal  $\text{H}^+$  secretion and, as a result,  $\text{HCO}_3^-$  reabsorption.

The  $\text{K}^+/\text{NH}_4^+$  antiporter has so far been observed only in mIMCD-3 cells and not in proximal tubule cells [15] or other nephron segments. Thus, this transporter may be unique to the inner medulla. Given the  $\text{K}^+$  and  $\text{NH}_4^+$  concentration gradients in the interstitium and the lumen of the inner medullary collecting duct cells and the non-ionic diffusion of  $\text{NH}_3$  at the luminal membrane, we suggest that this transporter is located in the basolateral membrane of inner medullary collecting duct cells and is likely responsible for the transport of  $\text{NH}_4^+$  from the interstitium to the cells of this nephron segment. Such a localization of  $\text{K}^+/\text{NH}_4^+$  antiporter in IMCD cells would provide, physiologically, an efficient mean of  $\text{NH}_4^+$  transport as well as  $\text{K}^+$  recycling in the inner medulla. Moreover,  $\text{NH}_4^+$  entrance via  $\text{K}^+/\text{NH}_4^+$  antiporter may also serve as a proton source for luminal  $\text{H}^+$  secretion and bicarbonate absorption. The latter possibility is suggested by studies in perfused cortical collecting tubules showing that total proton flux is greater in the presence of  $\text{NH}_4^+$  than its absence [47]. The inhibition of  $\text{K}^+/\text{NH}_4^+$  antiporter by verapamil which inhibits  $\text{K}^+$  channel [48] and by Sch-28080 which competes with the  $\text{K}^+$  binding site of the gastric  $\text{H}^+/\text{K}^+$ -ATPase [49] suggests that these agents may interact with the  $\text{K}^+$ -(or  $\text{NH}_4^+$ ) binding site of the  $\text{K}^+/\text{NH}_4^+$  antiporter. Finally, the  $\text{K}^+/\text{NH}_4^+$  antiporter is likely driven by an outwardly directed  $\text{K}^+$  concentration gradient generated and maintained by  $\text{Na}^+/\text{K}^+$  ATPase activity. Equilibrium thermodynamics predict that the  $\text{K}^+/\text{NH}_4^+$  antiporter will be at equilibrium and will mediate no net flux when

$[\text{K}^+]_i/[\text{K}^+]_o$  equals  $[\text{NH}_4^+]_o/[\text{NH}_4^+]_i$ . To determine the exact stoichiometry of  $\text{K}^+/\text{NH}_4^+$  antiporter (i.e. whether it is  $1\text{K}^+$  per  $1\text{NH}_4^+$  or whether there is a modifier site) one needs to measure intracellular  $\text{K}^+$  and  $\text{NH}_4^+$  concentrations in the presence of various outward  $\text{K}^+$  or inward  $\text{NH}_4^+$  gradients.

In conclusion, a new transporter, called  $\text{K}^+/\text{NH}_4^+$  antiporter, has been described in inner medullary collecting duct cells. This transporter exchanges intracellular  $\text{K}^+$  with extracellular  $\text{NH}_4^+$ , is inhibited by verapamil and Schering 28080, and is affected by physiologic alterations in  $\text{K}^+$  or  $\text{NH}_4^+$  concentrations. The  $\text{K}^+/\text{NH}_4^+$  antiporter may play an essential role in regulation of acid base balance.

## Acknowledgements

These studies were supported by the National Institute of Health Grant DK 46789, a Merit Review Grant from the Department of Veterans Affairs, and a grant from Dialysis Clinic Incorporated. The authors are very grateful to Dr. Charles Burnham for his contribution to these experiments. The authors acknowledge the technical assistance of Holli Shumaker. The critical review of the manuscript by Dr. John Galla is greatly appreciated.

## References

- [1] Knepper, M.A., Packer, R. and Good, D.W. (1989) *Physiol. Rev.* 69, 176–249.
- [2] Nagami G.T. and Kurokawa K. (1985) *J. Clin. Invest.* 81, 159–164.
- [3] Good, D.W., Knepper, M.A. and Burg, M.B. (1984) *Am. J. Physiol.* 247, F35–F44.
- [4] Good, D.W. and Knepper, M. (1985) *Am. J. Physiol.* 248, F459–F471.
- [5] Stern, L., Backman, K.A. and Hayslett, J. (1985) *Kidney Int.* 27, 652–661.
- [6] Good, D.W., Caflisch C.R. and DuBose, Jr. T.D. (1987) *Am. J. Physiol.* 252, F491–F500.
- [7] Preisig, P.A. and Alpern, R.J. (1990) *Am. J. Physiol.* 248, F459–F471.
- [8] Kinsella, J.L. and Aronson, P.S. (1981) *Am. J. Physiol.* 241, C220–C226.
- [9] Kinne, R., Kinne-Saffran, E., Schutz, H. and Scholermann, B. (1986) *J. Membr. Biol.* 94, 279–284.
- [10] Good, D.W. (1988) *Am. J. Physiol.* 255, F78–F87.
- [11] Kikeri, D., Sun, A., Zeidel, M.L. and Hebert, S.C. (1989) *Nature Lond.* 339, 478–480.

- [12] Amlal, H., Paillard, M. and Bichara, M. (1994) *Am. J. Physiol.* 267, C1607–C1615.
- [13] Wall, S.M. and Koger, L.M. (1994) *Am. J. Physiol.* 267, F660–F670.
- [14] Kurtz, I. and Balaban, R.S. (1986) *Am. J. Physiol.* 250, F497–F502.
- [15] Chen J.G. and Kempson S.A. (1993) *Biochim. Biophys. Acta* 1149, 299–304.
- [16] Wall, S.M., Trinh, H.N. and Woodward, K.E. (1995) *Am. J. Physiol.* 269, F536–F544.
- [17] Kikeri, D., Sun, A., Zeidel, M.L. and Hebert, S.C. (1992) *J. Gen. Physiol.* 99, 435–461.
- [18] Amlal, H., Paillard, M. and Bichara, M. (1994) *J. Biol. Chem.* 269, 1962–21972.
- [19] Soleimani, M., Singh, G., Bizal, G.L., Gullans, S.R. and McAteer, J.A. (1994) *J. Biol. Chem.* 269, 27973–27978.
- [20] Rauchman, M.I., Nigam, S.K., Delpire, E. and Gullans, S.R. (1993) *Am. J. Physiol.* 265, F416–F424.
- [21] Soleimani, M., Singh, G., Dominguez, J.H. and Howard, R.L. (1995) *Circ. Res.* 76, 530–535.
- [22] Singh, G., McAteer, J. and Soleimani, M. (1995) *Biochim. Biophys. Acta* 1239, 74–80.
- [23] Hargittati P.T., Youmans S.J. and Lieberman E.M. (1991) *Glia* 4, 611–616.
- [24] Waggoner, A. (1976) *J. Membr. Biol.* 27, 317–334.
- [25] Zeidel M.L., Kikeri, D., Silva, P., Burrowes, M. and Brenner, B.M. (1988) *J. Clin. Invest.* 82, 1067–1074.
- [26] Leviel, F., Borensztein, P., Houillier, P., Paillard, M. and Bichara, M. (1992) *J. Clin. Invest.* 90, 869–878.
- [27] Delpire, E., Rauchman M.I., Beier, D.R., Hebert, S. and Gullans, S.R. (1994) *J. Biol. Chem.* 269, 25677–25683.
- [28] Gamba, G., Miyanoshita, A., Lombardi, M., Lytton, J., Lee, W.S., Hediger, M.A. and Hebert, S.C. (1994) *J. Biol. Chem.* 269, 17713–17722.
- [29] Soleimani, M. and Singh, G., (1995) *J. Invest. Med.* 43, 419–430.
- [30] Hennessey, T. and Bradford, C.B. (1992) *J. Biol. Chem.* 267, 8161–8167.
- [31] Knepper, M.A., Good, D.W. and Burg, M.B. (1985) *Am. J. Physiol.* 247, F729–F738.
- [32] Wall, S.M. (1996) *Am. J. Physiol.* 270, F432–F439.
- [33] Graber, M. and Pastoriza-Munoz, E. (1993) *Am. J. Physiol.* 265, F773–F783.
- [34] Wingo, C.S. and Smolka, A.J. (1995) *Am. J. Physiol.* 269, F1–F16.
- [35] Younes-Ibrahim, M., Barlet-Bas, C., Buffin, M., Cheval, L., Rajerison, R. and Doucet, A. (1995) *Am. J. Physiol.* 268, F1141–F1147.
- [36] Kleinman, J.G., Tipnis, P. and Pscheidt, R. (1993) *Am. J. Physiol.* 265, F698–F704.
- [37] Shuichi, O., Guntupalli, J. and Dubose, Jr, T.D. (1996) *Am. J. Physiol.* 270, F852–F861.
- [38] Lauf, P.K., Bauer, J., Adragna, N.C., Fujise, H., Zade-Open, A.M.M., Ryn K.H. and Delpire, E. (1992) *Am. J. Physiol.* 263 (Cell Physiol. 32), C917–C932.
- [39] Greger, R. and Schlatter, E. (1983) *Pfluegers Arch.* 396, 325–334.
- [40] Warnock, D.G. and Eveloff, J. (1989) *Kidney Int.* 36, 412–417.
- [41] Light, D.B., McCann, F.V., Keller, T.M. and Stanton, B.A. (1988) *Am. J. Physiol.* 255 (Renal Fluid Electrolyte Physiol. 24), F278–F286.
- [42] Johnston, P.A., Battilana, A., Lacy, F.B. and Jamison, R.J. (1977) *J. Clin. Invest.* 59, 234–240.
- [43] Madias, N.E. and Perrone, R.D. (1988) Acid-base disorders in association with renal disease. In: *Diseases of the Kidney* (Schrier, R.W. and Gottschalk, eds.), pp. 2947–2981, Little, Brown and Co., New York.
- [44] Dubose, T.D. and Good, D.W. (1994) *J. Clin. Invest.* 90, 1443–1449.
- [45] Karlmark, B., Jaeger, P. and Giebisch, G. (1978) *Kid. Int.* 14, 766–772.
- [46] Soleimani, M., Bergman, J.A., Hosford, M.A. and McKinney, T.D. (1990) *J. Clin. Invest.* 86, 1076–1083.
- [47] Knepper, M.A., Good, D.W. and Burg, M.B. (1985) *Am. J. Physiol.* 249, F870–F877.
- [48] Bleich, M., Schlatter, E. and Greger, R. (1990) *Pfluegers Arch. Eur. J. Physiol.* 415, 449–460.
- [49] Wallmark, B., Briving, C., Fryklund, J., Munson, K., Jackson, R., Mandlein, J., Rabon, E. and Sachs, G. (1987). *J. Biol. Chem.* 262, 2077–2084.